AWESW2022
21st Australasian Wind Engineering Society Workshop
2 – 3 February, 2023

Investigation of Shielding Factors on Multiple Plane Frames at Various Solidities

Robert Reis[1], Jeung-Hwan Doh[1,2], Hassan Karampour[1,2], Matthew Mason[3]
[1]*Griffith School of Engineering and Built Environment, Griffith University, Gold Coast, Qld, Australia*
[2]*Cities Research Institute, Australia, Griffith University, QLD, Australia*
[3]*School of Civil Engineering, The University of Queensland, Brisbane, Qld, Australia*

ABSTRACT

As wind passes through a porous structure, such as a lattice frame or an unclad building, the drag force on the elements of the frame removes a portion of the energy of the flow and reduces the momentum. This in turn will reduce the force on subsequent frames and other elements downstream. Understanding this effect is important in enabling design of high-density open frame structures. Guidance on the shielding effects of upwind structural elements or frames on downwind elements is provided in AS/NZS1170.2:2021 "Structural Design Actions: Part 2 Wind Actions", based on work by the researchers Georgiou and Vickery in the late 1970's. The published data is based on wind tunnel testing on a series of identical parallel slat frames. With regards to unclad industrial structures, the work is useful in estimating the total wind force but has some shortcomings in that it assumes all the parallel frames are identical and that the frames are equally spaced. Using Computational Fluid Dynamics (CFD), a series of simulations has been undertaken to provide comparisons with AS/NZS 1170.2 and further development of guidelines to include the shielding effects of multiple frames at non-equal spacing. Preliminary results of this research indicate that CFD simulations may provide improved shielding calculations for industrial unclad structures.

1. Introduction

Structures encountered in mining, petrochemical and heavy industrial facilities include many which do not have external wall cladding yet present a high solidity due to the presence of processing equipment, piping, chute-work and storage vessels. It is of practical relevance to assess the effect of shielding from one structural frame (or structural "bay") to another to develop a conservative yet economic estimate of the total structure wind force.

In this study a comparison of the wind forces generated by a flow on two surface mounted plates in tandem has been undertaken using values obtained from AS/NZS1170.2 "Structural Design Actions: Part 2 Wind Actions" Standards Australia & Standards New Zealand (2021) (AS/NZS1170.2) based calculations and Computational Fluid Dynamics (CFD) simulations using the Scale Adaptive Simulation turbulence model in ANSYS Fluent V21. The solidity of the windward plate was varied from 50 to 100% to simulate different framing solidities while the leeward plate was maintained at 100% solidity for all tests. The spacing between the windward and leeward plates was varied as a function of the plate width. The high framing solidities were selected to focus on high solidity open frame structures as found on mining and industrial sites as compared with low solidity lattice frames found in transmission towers. From AS/NZS 1170.2 Supplement 1:2002 "Structural design actions – Wind actions – Commentary", Standards Australia (2002) (AS/NZS1170.2 Commentary), the shielding factors adopted in the Australian Standard were derived from studies undertaken by Georgiou & Vickery (1979). This

study utilised identical parallel slatted frames mounted on a force balance within a wind tunnel as shown in Figure 1.

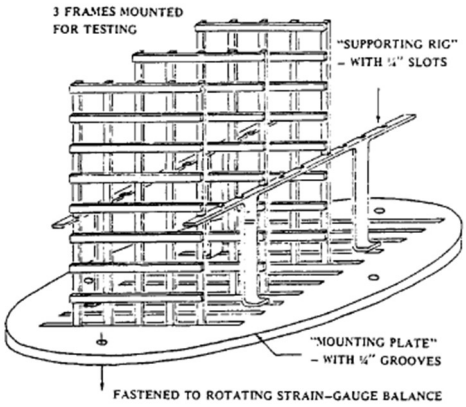

Figure 1 Georgiou Vickery Apparatus - Georgiou & Vickery (1979)

This research has identified three improvements to the original work. Firstly, the arrangement of a single force balance does not provide insight as to the force components of each frame, only the total force. Secondly, the arrangement does not provide a measure of the total shielding effect from the first frame, only the influence on the second and subsequent identical frames. Finally, the effect of unequal spacings was not explored.

While there is still work to be done in validating the overall accuracy of CFD tools, the drag forces can be estimated as discussed by Thordal, Bennetsen, & Koss (2019). There is a strong attraction to their use in providing the improvements noted above which may be time consuming and technically challenging to achieve using wind tunnel techniques.

There is a practical need for this research given the potential improvements identified above and the potential insights that can be gained by adopting a different modelling/analysis approach. The benefits include both improved safety to personnel working at such facilities and the surrounding public, and in providing economical designs. The methodology and results of this early phase work are presented in this paper.

2. Analytical Model

For the CFD simulation it was necessary to select an appropriate wind speed. In the Australian context the largest forces required to be withstood by a structure are for the ultimate (strength) limit state. Referencing the National Construction Code, Australian Building Codes Board (2019) (NCC) and AS/NZS 1170.2, for a typical non-cyclonic environment the design wind speed was estimated based on the criteria in Table 1. (Note: The equations provided following are based on those from AS/NZS1170.2 but have been modified to suit the specific details of this research, however the nomenclature has been kept consistent.)

Table 1 Design wind speed derivation

Importance Level	NCC Table B1.2a	2 - Normal Structures
Design Events for Safety	NCC Table B1.2b	1:500 – Non-Cyclonic
Wind Region	AS/NZS 1170.2 Figure 1.3(A)	A – Non-Coastal, Non-Cyclonic
Regional Wind Speed, V_R	AS/NZS1170.2 Table 3.1(A)	45 m/s
Terrain/Height Multiplier, $M_{z,cat}$	AS/NZS1170.2 Table 4.1	1.12 (Less than 30m)

Values for AS/NZS1170.2 parameters for M_c, M_d, M_s, M_t all taken as 1.0

The design wind speed is then given by:

$$V_{des} = V_R\, M_c\, M_d\, (M_{z,cat}\, M_s\, M_t) \quad (1)$$

Resulting in a design wind speed of 50 m/s. Details of the analytical model are provided in Table 2 with the geometry shown in Figure 2.

Table 2 Model details

Plate Height	c	24 m
Plate Width	b	24 m
Aspect Ratio	b/c	1
Plate Thickness	t	0.6m
Plate Spacings	In terms of b	$0.5b, b, 2b, 3b, 4b$
Gross Plate Area	$A_g = b \times c$	576 m^2
Windward Plate Solidity Ratios	δ = Solid Area / Gross Area	50%, 70%, 80%, 90%, 100%

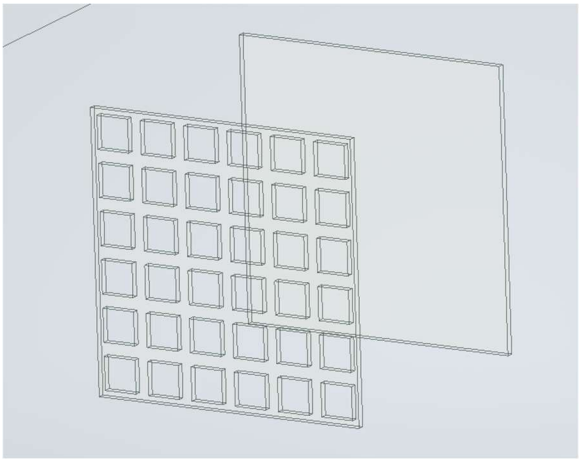

Figure 2 CFD Geometry showing 50% solidity windward plate and solid leeward

The plate spacings are a subset of the values provided in AS/NZS 1170.2 Table C.2, noting that frame spacing ratios of less than 0.2 and greater than 8.0 are unlikely to be encountered regularly. The solidity ratios chosen were selected to target the higher end of AS/NZS 1170.2 Table C.2 where a gap analysis showed there is limited data. The existing data consistently indicated high shielding which was thought to provide a good basis for validation of CFD modelling. For this analysis, the Reynolds Number is of the order of 81 x 10^6.

3. AS/NZS 1170.2 Force and Shielding Calculations

The design wind pressure for the force calculation is given by:

$$p = (0.5\rho_{air})[V_{des}]^2 \quad (2)$$

Using the density of air, ρ_{air} = 1.225 kg/m^3, the design pressure p = 1.53 kPa is obtained.
The pressure coefficient for the plate is similar to a free standing wall as provided in AS/NZS 1170.2 Table B.2(A) following the work of Letchford & Holmes (1994) and given by:

$$C_{pn} = 1.3 + 0.5[0.3 + log_{10}(b/c)](0.8 - c/h) \quad (3)$$

Given h = 0 for a surface mounted plate, the pressure coefficient, $C_{p,n}$ = 1.27.

To account for the variation in windward plate solidity, the area of the plate was adjusted using a porosity factor given by:

$$K_p = 1 - (1 - \delta)^2 \tag{4}$$

It was suggested by Cook (1999) that at higher solidities (δ > 0.8), the "lattice" becomes a porous wall as more flow is forced around than through the frame. Therefore, the total force on an unshielded plate is given by:

$$F_{un} = K_p \, C_{p,n} \, A \, p \tag{5}$$

The shielding factors, K_{sh} are then obtained from Table C.2 of AS/NZS 1170.2 using the solidity ratio δ and the frame spacing ratio, λ based on the centre-to-centre frame spacing divided by the width b. The calculated forces are shown in Table 3.

4. CFD Methodology

Conceptually, a CFD simulation domain is analogous to a wind tunnel and some key considerations in wind tunnel testing also apply for CFD when comparing to the real world. The flow is confined within the domain and there is a finite amount of fluid (air) within the domain. The blockage created by the test model will increase the velocity due to continuity of momentum, and correspondingly the dynamic pressure, within the domain resulting in a force increase. This is accounted for primarily by ensuring that the maximum blockage ratio is below 5%. As such the side and top offsets of the domain from the plate were adjusted to achieve the 5% limit resulting in a total domain width of 144m (6 x plate height c) and 84m high (3.5 x c). A further adjustment was made within the final results based on the domain averaged accelerated flow velocity at the blockage.

To expedite the simulations, the domain extents were reduced to reduce the cell count. A sensitivity analysis was undertaken to ensure that the reduced lengths did not adversely affect the results. An inlet length of 48m (2 x c) and outlet length behind second plate of 120m (5 x c). The impact of this approach is that with the short inlet length a fully developed turbulent boundary layer is not established. Apart from a small boundary layer of 2m in height with a velocity drop of approximately 5%, the flow is effectively laminar approaching the plates. These values were obtained from a simulation of an empty domain. An adjustment has been made to the final results by adjusting the force values using a ratio calculated from the average dynamic pressure for an equivalent AS/NZS 1170.2 Terrain Category 2 boundary layer to the constant 50m/s dynamic pressure.

Prior to undertaking the simulations, a mesh convergence study was undertaken to confirm the mesh sizing. This involved a structured refining of the mesh to determine a sizing regime where the mesh size did not vary the results significantly. For the study, a steady Reynolds Averaged Navier Stokes (RANS) precursor simulation was undertaken using the kω-SST turbulence model in line with recommendations by Gerasimov (2016). Given the models are highly unsteady and do not converge using typical convergence criteria, the simulations were run with sufficient iterations until the mean force values remained constant. It was found that the criteria of 20 cells across of characteristic dimension provided a stable result following the guidelines of Menter (2015). The boundary conditions of the domain consisted of a velocity inlet with a uniform 50 m/s flow, a pressure outlet, no-slip wall for the ground plane, and free slip walls and top.

It was anticipated from the outset that an unsteady solution would be required due to the periodic fluctuations behind the plates which would prevent convergence of a steady solution following Mochidaa, Tominagab, & Yoshiec (2006). For the turbulence model, the Scale Adaptive Simulation

(SAS) model of Menter & Egorov (2010) was used. This model was selected following review of similar works including that of Poulain, Craig, & Meyer (2021) showing that it produced acceptable drag force results for bluff body flow while being computationally affordable. This discussion will not attempt to cover the detail of the SAS model, however it has been developed specifically to account for flows with strong instabilities associated with separation zones behind bluff bodies. The numerical settings for the simulations follow the guidelines of Menter (2015). The time step size was calculated by maintaining a Courant number of 1 for the smallest calculated cell size and the free stream velocity, V_{des}. The duration was set to 20 seconds of flow time, of which the latter 15 seconds was used for sampling the forces, ignoring the first 5 seconds for flow field stabilisation. In summary the solution was based on 16000 steps at 0.00125 seconds per step. The force values shown in the results are mean values for the 15 seconds.

5. Results and Discussion

The results for the single plate models at various solidities is presented in Table 3 and Figure 3. The Effective Pressure Coefficient was obtained by dividing F_{un} by both the solid plate area, A_g and the dynamic pressure, p.

Table 3 Single Plate Forces of leeward plate

Windward Plate Solidity Ratio (%)	Plate Force, F_{un} (kN)		Effective Pressure Coefficient, C_{pe}		Variation (%)
	AS/NZS1170.2	CFD*	AS/NZS1170.2	CFD*	
50	840	599	0.95	0.68	-28.7
70	1019	813	1.16	0.92	-20.2
80	1075	921	1.22	1.04	-14.3
90	1109	1039	1.26	1.18	-6.3
100	1120	1148	1.27	1.30	2.5

* Mean values averaged over simulation time and adjusted for blockage and boundary layer effects

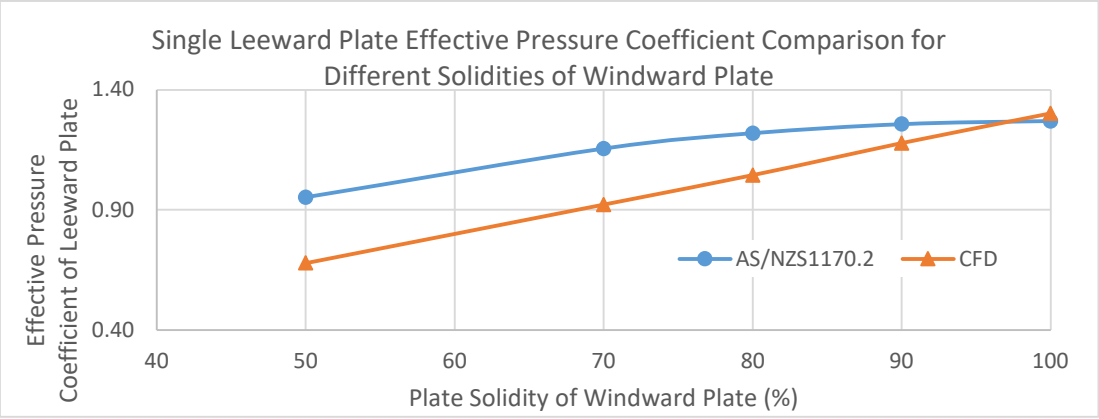

Figure 3 Single Plate Effective Pressure Coefficients

In reviewing the results, for the solid plate case, at 100% solidity the AS/NZS1170.2 and CFD results are well aligned with 2.5% variation. The results diverge as the solidity decreases with a variation of up to 28.7% for the 50% solidity case. Interestingly in this high solidity range investigated, the CFD indicates a linear relationship between plate solidity and effective pressure coefficient. The potential of this simple linear coefficient will be investigated on future stages of this research. The curved result for the AS/NZS 1170.2 results can be explained by the squared term in the calculation of K_p. The transition point from low solidity flow regime to high solidity indicated by Cook (1999) at around 80% solidity is not evident in the CFD results. The velocity profiles shown in Figure 4 shows separation and

recirculation zone between 2 and 3 plate height spacings. Whereas the 50% solidity case indicates a lowered velocity profile for a significant distance downwind. This variation is likely to produce vastly different shielding effects for the different solidities in the two plate models.

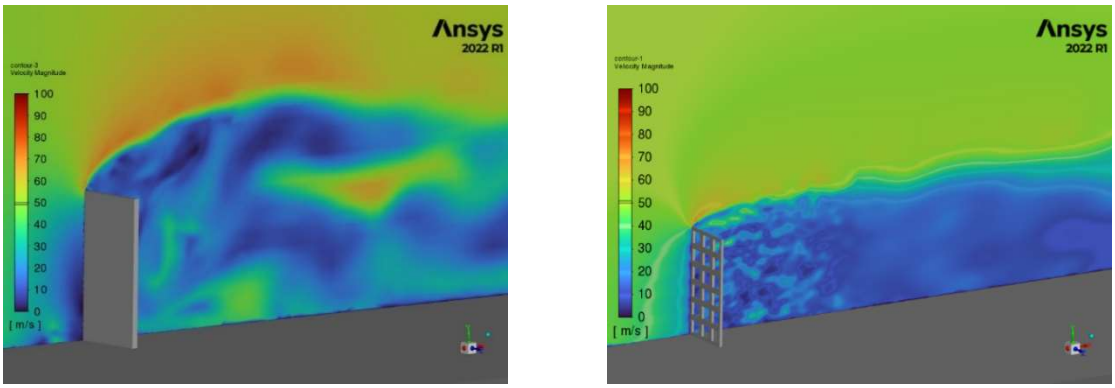

Figure 4 Velocity profiles for the 100% solidity and 50% solidity cases

6. Conclusions

One of the specific advantages of using CFD is the ability to monitor the force for each plate. This can provide an insight into the drivers of the shielding effects for both spacing and solidity. Given the close alignment of the 100% solidity plate values from CFD when compared to AS/NZS1170.2, there is potential for further research to fill the identified gaps and improve the current published guidance regarding calculation of shielding factors for unclad industrial structures.

References

Australian Building Codes Board. (2019). National Construction Code Volume 1 (Vol. NCC 2019 Volume 1). Canberra, Australia: Australian Building Codes Board.

Cook, N. J. (1999). Wind loading: A practical guide to BS 6399-2, Wind loads on buildings. London: Thomas Telford Publishing.

Georgiou, P. N., & Vickery, B. J. (1979). *Wind Loads on Building Frames*. Paper presented at the Wind Engineering - Proceedings of the Fifth International Conference, Fort Collins, Colorado, USA.

Gerasimov, A. (2016). Quick Guide to Setting Up LES type Simulations. 50. Retrieved from https://support.ansys.com

Letchford, C. W., & Holmes, J. D. (1994). Wind loads on free-standing walls in turbulent boundary layers. *Journal of Wind Engineering and Industrial Aerodynamics, 51*(1), 1-27. doi:https://doi.org/10.1016/0167-6105(94)90074-4

Menter, F. R. (2015). Best Practice: Scale-Resolving Simulations in ANSYS CFD. Retrieved from https://support.ansys.com

Menter, F. R., & Egorov, Y. (2010). The Scale-Adaptive Simulation Method for Unsteady Turbulent Flow Predictions. Part 1: Theory and Model Description. *Flow, Turbulence and Combustion, 85*(1), 113-138. doi:10.1007/s10494-010-9264-5

Mochidaa, A., Tominagab, Y., & Yoshiec, R. (2006). AIJ Guideline for Practical Applications of CFD to Wind Environment around Buildings. Paper presented at the *The Fourth International Symposium on Computational Wind Engineering*, Yokohama, Japan.

Poulain, P., Craig, K. J., & Meyer, J. P. (2021). Transient simulation of an atmospheric boundary layer flow past a heliostat using the Scale-Adaptive Simulation turbulence model. *Journal of Wind Engineering and Industrial Aerodynamics, 218*. doi:10.1016/j.jweia.2021.104740

Standards Australia. (2002). AS/NZS 1170.2 Supplement 1:2002 Structural design actions - Wind actions - Commentary (Vol. AS/NZS 1170.2 Supp 1:2002). Sydney: Standards Australia.

Standards Australia & Standards New Zealand. (2021). AS/NZS 1170.2:2021 Structural Design Actions: Part 2 Wind Actions: SAI Global.

Thordal, M. S., Bennetsen, J. C., & Koss, H. H. H. (2019). Review for practical application of CFD for the determination of wind load on high-rise buildings. *Journal of Wind Engineering and Industrial Aerodynamics, 186*, 155-168. doi:10.1016/j.jweia.2018.12.019